PNAS
www.pnas.org

Supplementary Information for

Metal ions confinement defines the stacking mode of G-quartet, the conformation of G-quadruplex fibrils and their assembly into nematic tactoids

Xiaoyang Li[a,b], Antoni Sánchez-Ferrer[b,c], Massimo Bagnani[b], Jozef Adamcik[b], Paride Azzari[b], Jingcheng Hao[a,1], Aixin Song[a], Hongguo Liu[a] & Raffaele Mezzenga[b,d,1]

[a]Key Laboratory of Colloid and Interface Chemistry & State Key Laboratory of Crystal Materials, Shandong University, Jinan, Shandong 250100, China;
[b]Department of Health Science and Technology, ETH Zurich, Zurich 8092, Switzerland;
[c]Wood Research Munich (HFM), Technical University of Munich, Munich 80797, Germany;
[d]Department of Materials, ETH Zurich, Zurich 8093, Switzerland

[1]Email: jhao@sdu.edu.cn, or raffaele.mezzenga@hest.ethz.ch.

This PDF file includes:

Supplementary Materials and Methods

Preparation of G-quadruplex hydrogels.

GB was prepared as a G-assemblies precursor by mixing guanosine (0.028 g, 0.1 mmol), phenylboronic acid (0.012 g, 0.1 mmol) and sodium hydroxide (0.004 g, 0.1 mmol) in water (2 mL) and heated to 80 ^{o}C for 2 h. In order to obtain hydrogels, four types of salts (KCl, $CaCl_2$, $SrCl_2$, $BaCl_2$) at different concentrations were added to GB aqueous solutions, which were then slowly cooled down to room temperature.

Circular dichroism.

Circular dichroism (CD) measurements were performed on a J-815-150S spectrometer, equipped with a Peltier controlled cell holder. Signals were recorded from 340 nm to 220 nm with a scan speed of 100 nm min^{-1} and band width of 1 nm at 20 ^{o}C. Due to the strong CD signals, the path length of the quartz plate was fixed at about 0.01 mm.

Small- and wide-angle X-ray scattering.

Small and wide-angle X-ray scattering (SAXS and WAXS) intensity profiles were acquired on a Rigaku MicroMax-002^{+} (Tokyo, Japan) equipped with a microfocused beam (40 W, 45 kV, 880 μA) and with the $\lambda_{Cu\ K\alpha}$ = 0.15418 nm radiation collimated by three pinhole collimators (0.4, 0.3, and 0.8 mm). The diffracted X-rays were collected by a two-dimensional (2D) Triton-200 gas-filled X-ray detector and a 2D Fujifilm BAS-MS 2025 (Fujifilm, Japan) imaging plate system. The scattering wave vector q, which is defined as $q = 4\pi\sin(\theta)/\lambda_{Cu\ K\alpha}$ with a scattering angle of 2θ, was obtained in a range of 0.05 nm^{-1} < q < 25 nm^{-1}. Samples used for WAXS measurements were freeze-dried hydrogels and for SAXS were hydrogels without any further treatment.

Rheological measurements.

Rheological properties of hydrogels were measured on a AR2000 rheometer (TA Instruments) with stainless steel cone and plate geometry (diameter 20 mm and angle 2°) with a truncation gap of 59 μm. Hydrogels were put on the plate and were measured at 25 ^{o}C with the help of a circulating water bath. The oscillatory stress sweeps were measured to obtain the linear viscoelastic region with an angular frequency of 1 rad s^{-1} and a stress range 0.01-100 Pa. To evaluate the mechanical stiffness of hydrogels, the storage modulus G' was obtained from the oscillatory frequency sweeps in an angular frequency range 0.001-100 Hz with a stress set value obtained from the linear viscoelastic region in the oscillatory stress sweep. All samples were measured three times individually and the error bars in plots represent the standard deviations. Shear-recovery experiments were performed by a gradual increase of shear rate from 10^{-2} to 10^{3} s^{-1} and a following decrease from 10^{3} to 10^{-2} s^{-1}.

Atomic force microscopy.

Atomic force microscopy (AFM) were performed on a Nanoscope VIII Multimode Scanning Force Microscope (Bruker, USA) in tapping mode. For an effective immobilization of samples on mica surface, APTES was used to modify the mica surface to a positively charged mica substrate (AP-mica). Because fibrils featured by G-quadruplex structures are negatively charged, APTES aqueous solution (0.05 %-V/V) was deposited on a cleaved mica surface, incubated for 1 min, washed with 1 mL MilliQ water for three times, and dried by pressurized air. 20 μL samples were deposited onto AP-mica, incubated for 30 s, washed with 1 mL Milli-Q water, and dried by pressurized air. NanoscopeAnalysis 1.5 was used for the image processing. FiberApp, an open-source software, was used for the statistical analysis of the fibrils, including the height distribution and the pitch of twisted fibrils.

Preparation of liquid crystalline droplets and characterization by LC Polscope.

Guanosine, phenylboronic acid and potassium hydroxide were added in water with a molar ratio of 1:1:1 and heated to 80 ^{o}C for 2 h until all chemicals dissolved. Solutions were then cooled down slowly to room temperature to obtain hydrogels. The birefringence determination of samples was first performed by cross-polarizers to identify the liquid-crystalline phase. For the analysis of liquid crystalline droplets, a LC Polscope universal compensator mounted on a Zeiss Axioscope 2 microscope with 5× and 10× objectives, was used. For the observation under the microscope, the sample was inserted into two microscope slides and sealed with epoxy glue. After curing of the epoxy glue the samples were heated to 80 ^{o}C and successively cooled down slowly to room temperature for final observation.

Supplementary Figures

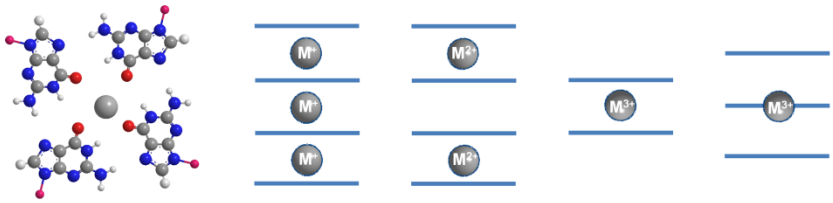

Fig. S1. Common binding modes of metal ions with different charges in the G-quadruplex channels. Each bar stands for a G-quartet plane as shown in the left.

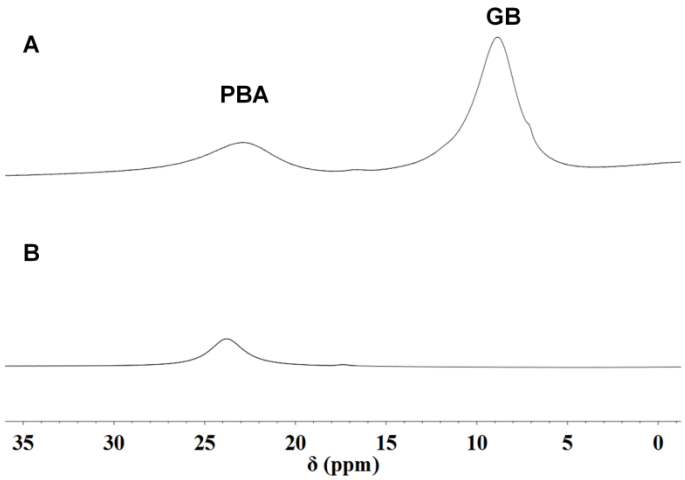

Fig. S2. ^{11}B NMR spectra of **GB** (A) and **PBA** (B) in D_2O at the same pH. **GB** was prepared by the reaction of **G**, **PBA** and sodium hydroxide with a molar ratio of 1:1:1. The pH of **PBA** aqueous solution was modulated by sodium hydroxide. Two peaks appear at 8.8 and 22.9 ppm in ^{11}B NMR spectra of **GB** aqueous solution, which should be attributed to borate monoester **GB** and unreacted **PBA**, respectively, confirming the formation of **GB**.

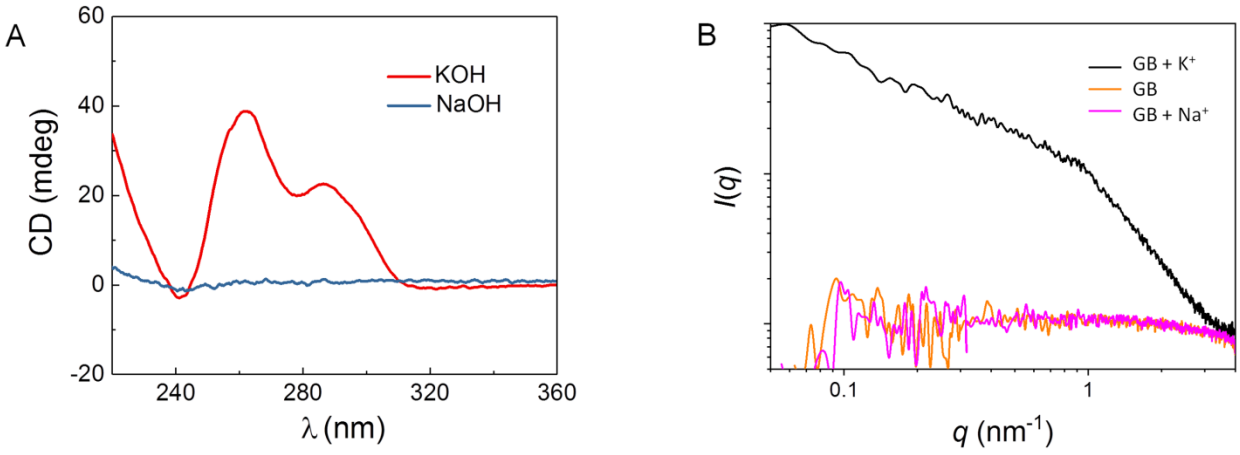

Fig. S3. Sample formed with only Na^+ cannot form G-quadruplex. (A) CD spectrum of sample formed by guanosine, phenylboronic acid and NaOH shows no G-quadruplex signals. Sample with KOH (red curve) instead of NaOH (blue curve) shows significant signals, which are characteristic of G-quadruplex. (B) SAXS intensity profiles of GB aqueous solution formed by guanosine, phenylboronic acid and NaOH (orange curve), as well as a GB sample with adding excess NaCl (pink curve), showing no scattering signal. The result suggests no G-quadruplex formation by the template of only Na^+, while the GB sample with the addition of K^+ (black curve) shows scattering signal.

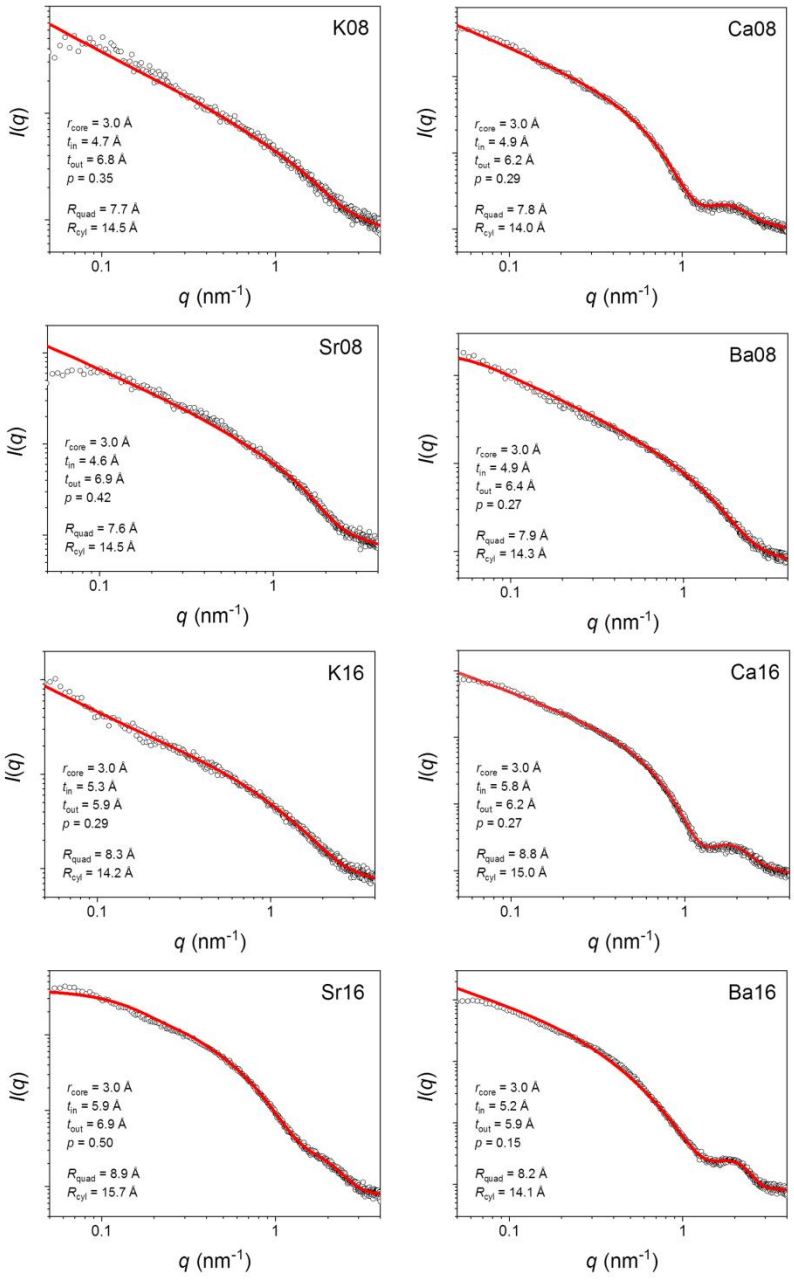

Fig. S4. SAXS intensity profile of the hydrogels formed by adding K^+, Ba^{2+}, Sr^{2+} and Ca^{2+} at 8 and 16 mM together with the corresponding fitting curve in red. The concentration of **GB** is 50 mM.

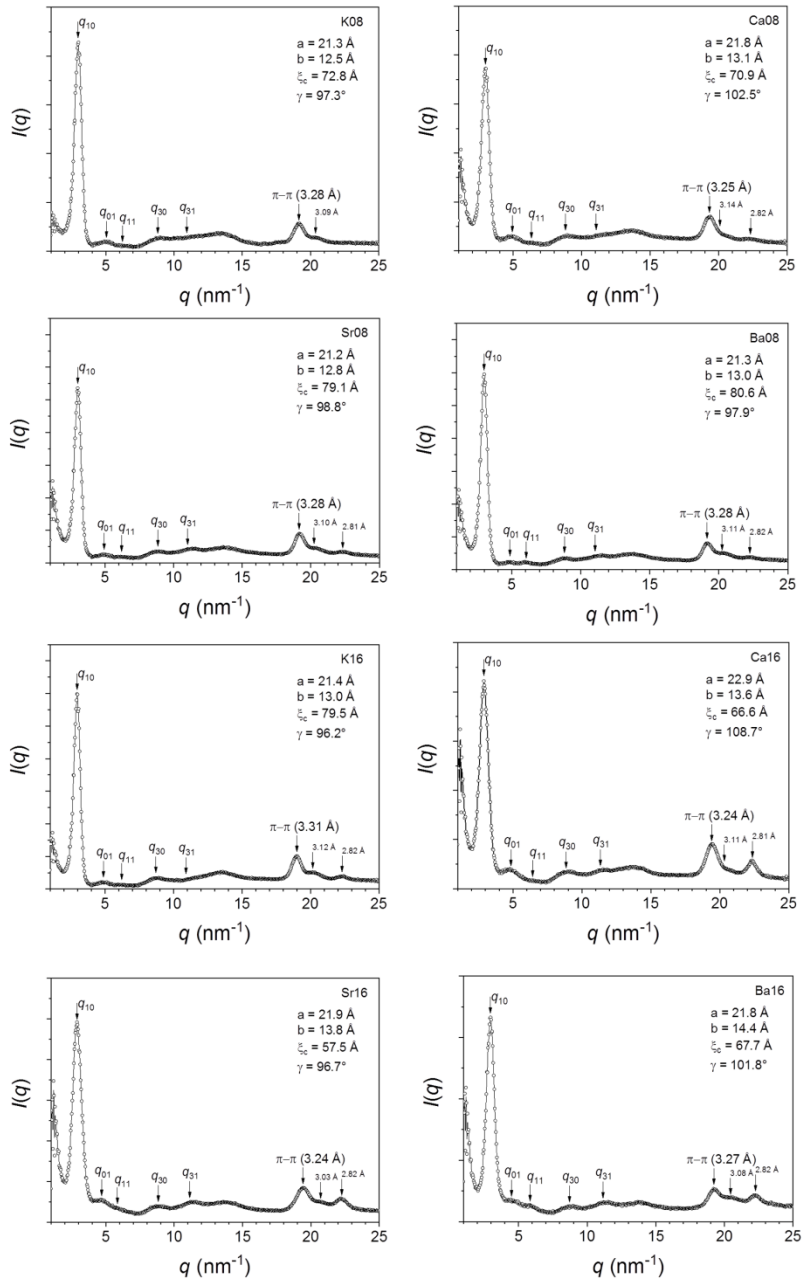

Fig. S5. WAXS intensity profile of the freeze-dried hydrogels formed by adding K^+, Ba^{2+}, Sr^{2+} and Ca^{2+} at 8 and 16 mM. The concentration of **GB** is 50 mM.

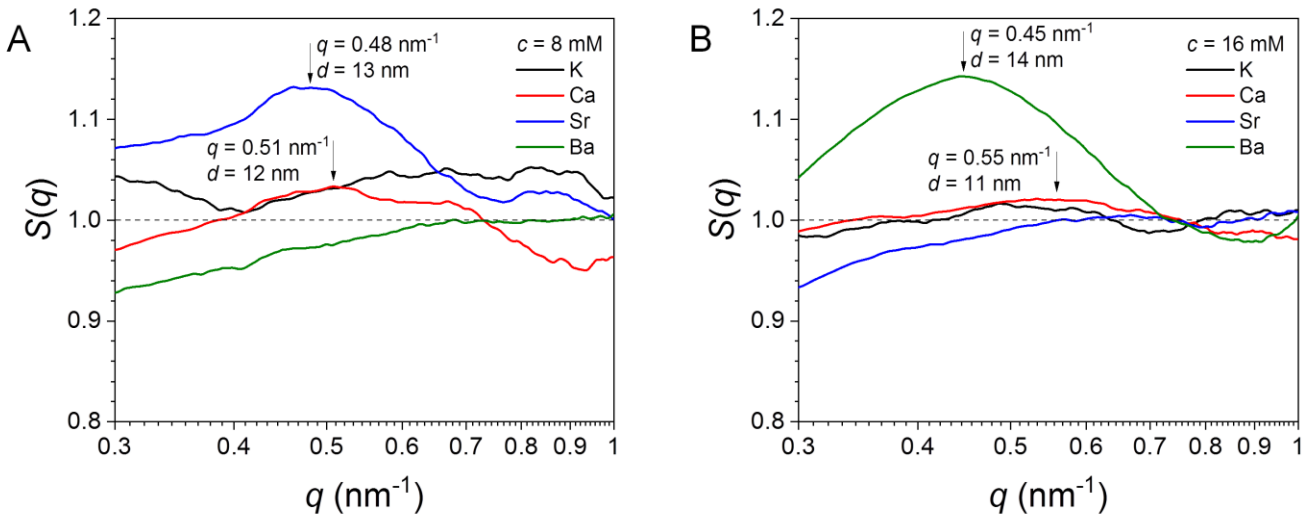

Fig. S6. Structure factor S(q) of the hydrogels formed by adding K^+, Ba^{2+}, Sr^{2+} and Ca^{2+} at 8 (A) and 16 mM (B). The concentration of **GB** is 50 mM.

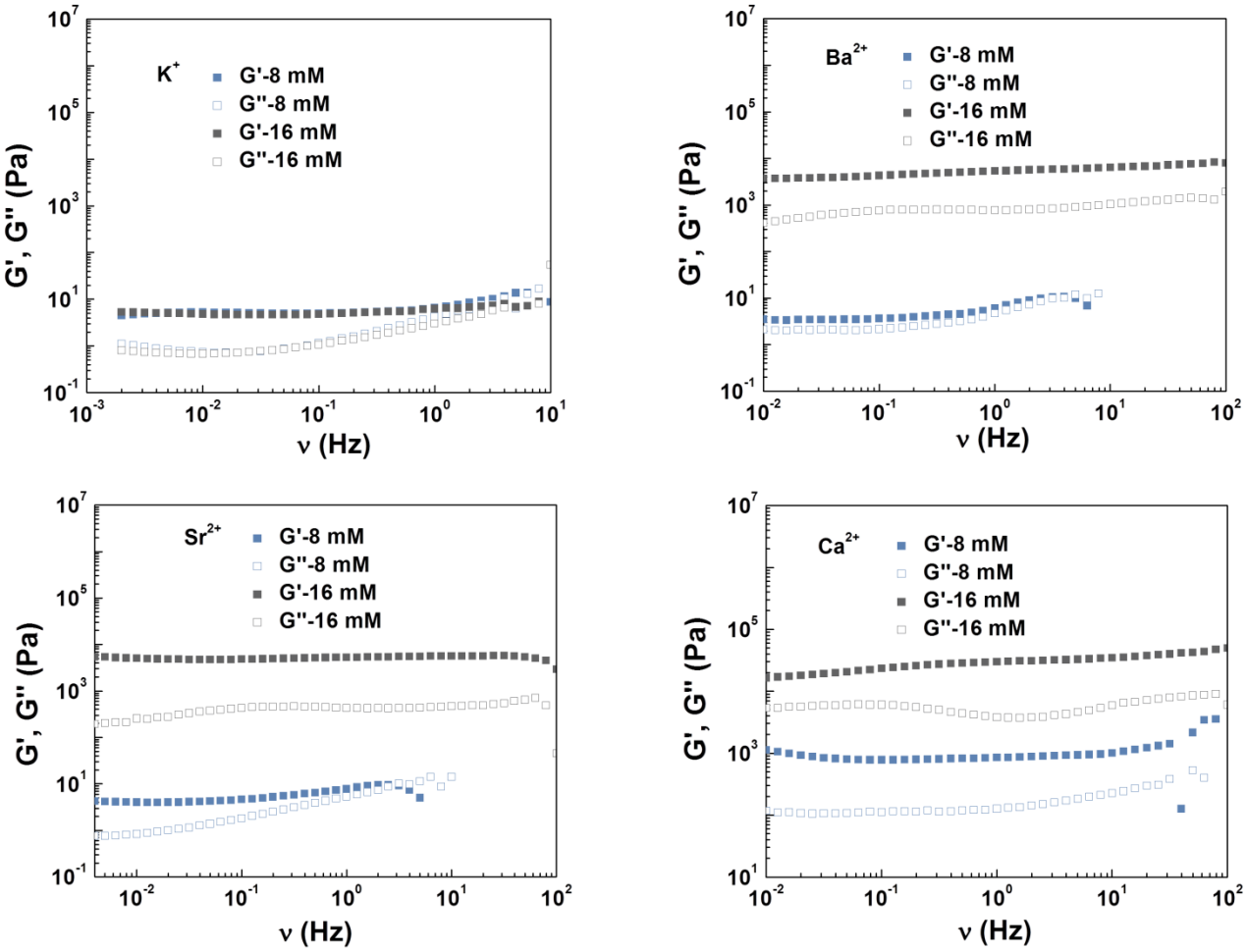

Fig. S7. Oscillatory frequency sweep of hydrogels formed by adding K^+, Ba^{2+}, Sr^{2+} and Ca^{2+} at 8 (blue symbols) and 16 mM (black symbols). The concentration of **GB** is 50 mM.

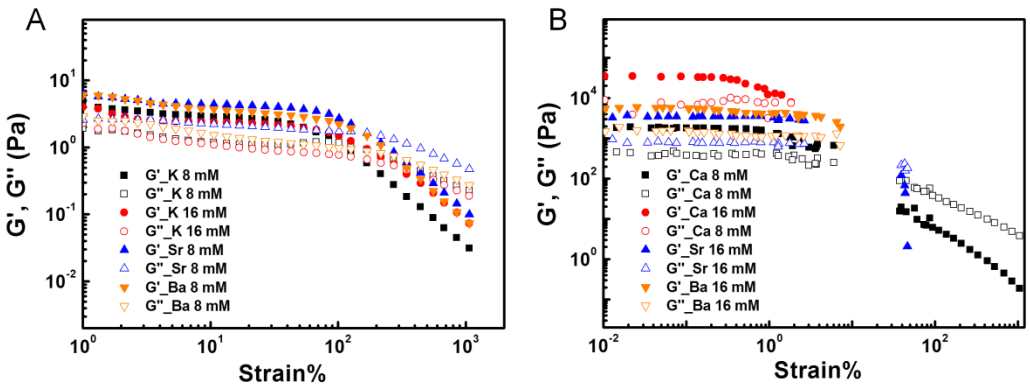

Fig. S8. Strain sweeps on hydrogels formed with four metal ions at two different concentrations (8 mM and 16 mM) at 20 °C. The concentration of **GB** is 50 mM.

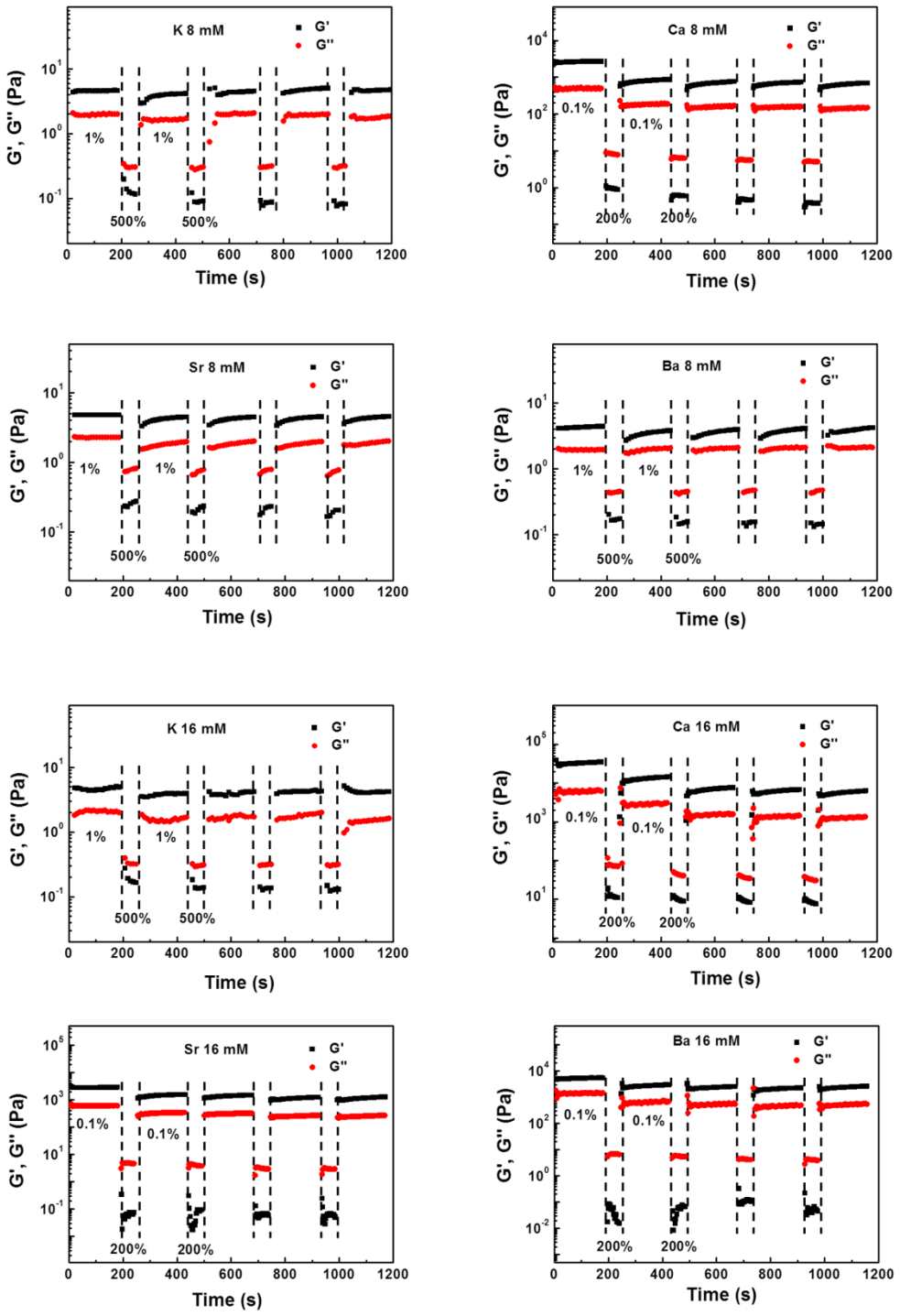

Fig. S9. Continuous strain step experiments on hydrogels formed with four metal ions at two different concentrations (8 mM and 16 mM) at 20 °C. The concentration of **GB** is 50 mM.

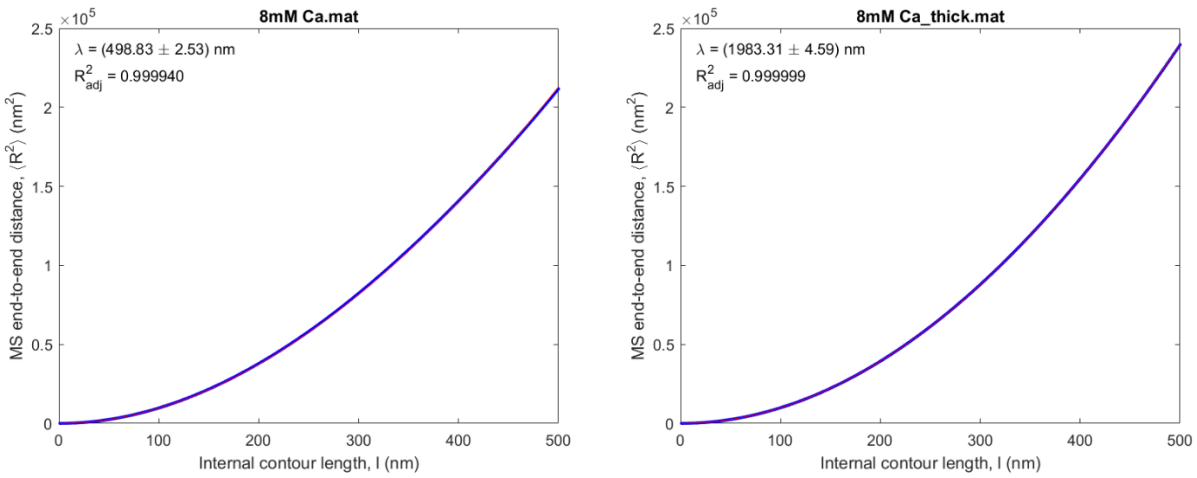

Fig. S10. Persistence length estimation for fibrils formed with Ca^{2+} at 8 mM (corresponding to Fig. 3*A*) by the 2D worm-like chain model. In the case of 8 mM Ca^{2+}, there are both thin and thick fibrils. The persistence length of thin fibrils is similar to that of fibrils formed by 8 mM K^{+}, and it is ca 500 nm. For the thick fibrils in the case of Ca^{2+}, the persistence length is about 2 μm.

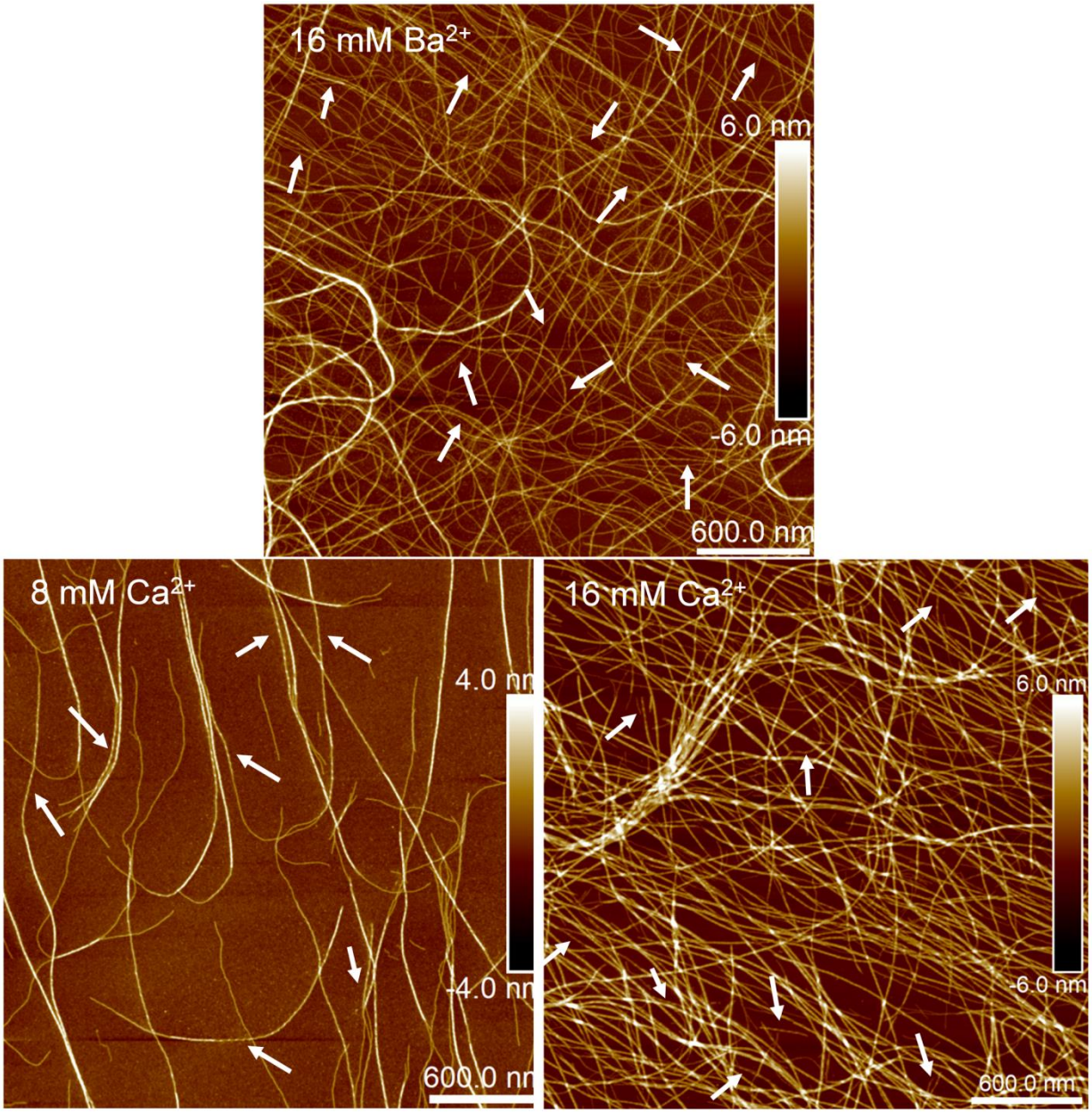

Fig. S11. The detailed AFM images of hydrogels formed by adding 16 mM Ba^{2+}, 8 and 16 mM Ca^{2+} corresponding to images with left-handed twisted fibrils in Figure 3.

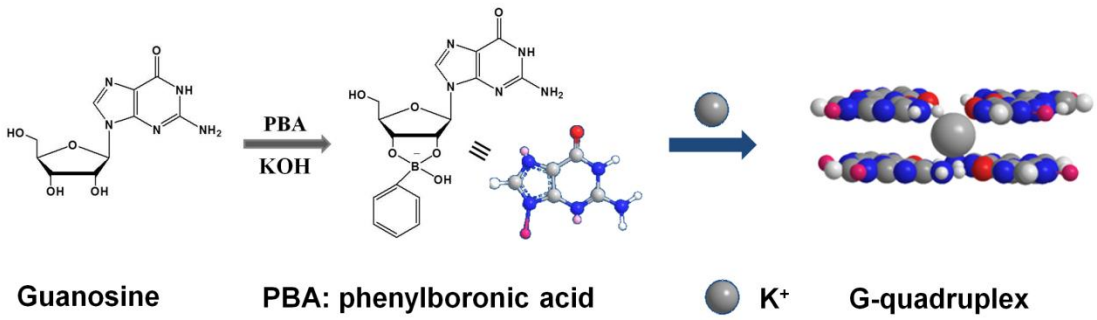

Fig. S12. Preparation of G-quadruplex hydrogels by the reaction of guanosine, **PBA** and KOH.

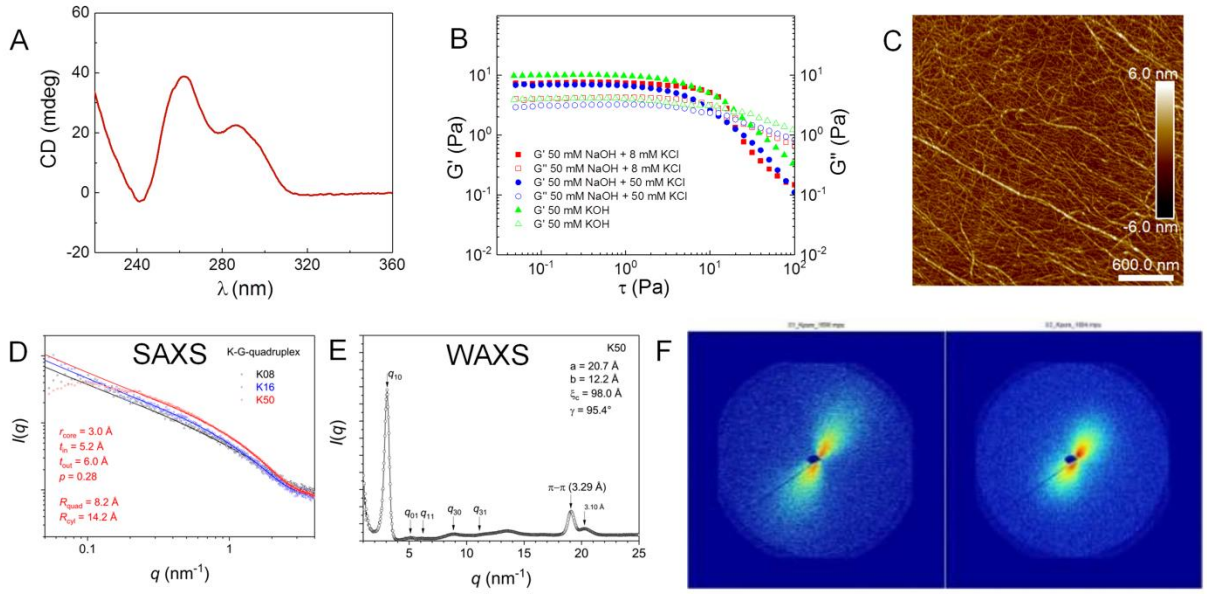

Fig. S13. Characterization of hydrogels formed by guanosine, PBA and KOH at 40 mM: (A) the CD spectrum; (B) the oscillatory stress sweep; (C) AFM image; (D) SAXS and (E) WAXS results; (F) 2D SAXS pattern.

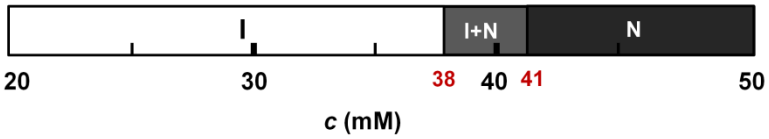

Fig. S14. The phase diagram of G-quadruplex hydrogels plotted against guanosine concentration. The molar ratio of guanosine, PBA and KOH is fixed at 1:1:1. I and N represent isotropic and nematic phase, respectively. A biphasic regime (isotropic and nematic phase) was formed in the concentration range of 38 - 41 mM.

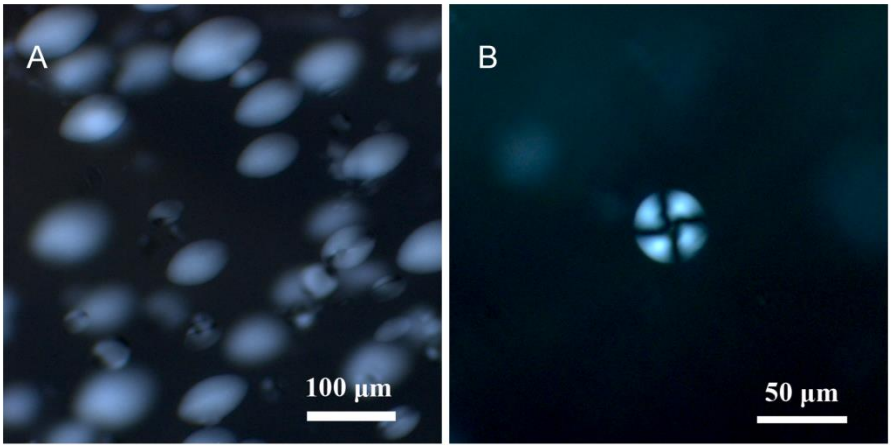

Fig. S15. Cross-polarized microscope images of homogeneous nematic tactoids (A) and radial nematic tactoids (B). The concentration of **G**, **PBA** and KOH are 40 mM.

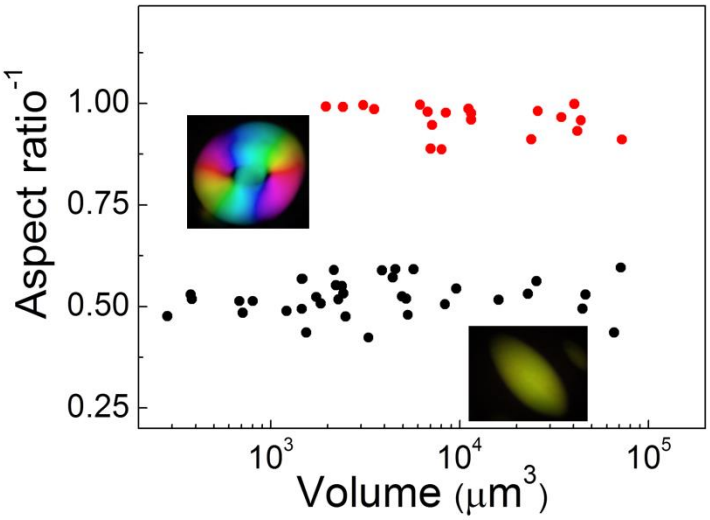

Fig. S16. The reciprocal of aspect ratio of **tactoids** as a function of their volumes. The red symbols represent droplets in a radial configuration, and the black symbols represent homogeneous tactoids. The tactoids were formed with **G**, **PBA** and KOH at 40 mM.

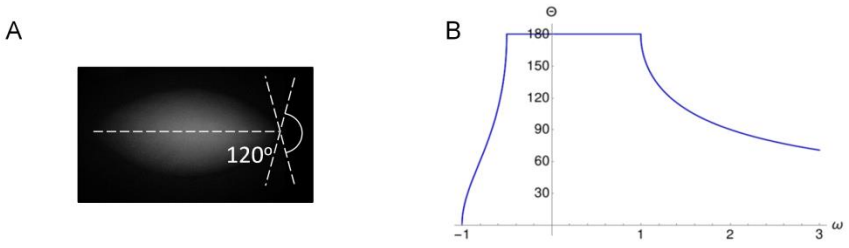

Fig. S17. (A) Picture showing the tip angle measurements on homogeneous tactoids. (B) The tip angles of tactoids as a function of the anchoring strength in Wulff construction.

Supplementary Tables

Table S1. Core radius (r_{core}), inner (t_{in}) and outer (t_{out}) shell thickness, polydispersity (p) and quadruplex (D_{quad}) and cylinder (D_{cyl}) diameter of the hydrogels formed by adding K^+, Ba^{2+}, Sr^{2+} and Ca^{2+} at 8 and 16 mM.

Sample	r_{core} (Å)	t_{in} (Å)	t_{out} (Å)	p	D_{quad} (Å)	D_{cyl} (Å)
K08	3.0	4.7	6.8	0.35	15.4	29.0
Ca08	3.0	4.9	6.2	0.29	15.7	28.1
Sr08	3.0	4.6	6.9	0.42	15.2	29.0
Ba08	3.0	4.9	6.4	0.27	15.7	28.6
K16	3.0	5.3	5.9	0.29	16.6	28.4
Ca16	3.0	5.8	6.2	0.27	17.6	29.9
Sr16	3.0	5.9	6.9	0.50	17.7	31.4
Ba16	3.0	5.2	5.9	0.15	16.3	28.2

Table S2. Lattice parameters (a, b, γ) and π-π stacking distance ($d_{\pi-\pi}$) of the freeze-dried hydrogels formed by adding K^+, Ba^{2+}, Sr^{2+} and Ca^{2+} at 8 and 16 mM.

Sample	a (Å)	b (Å)	γ (deg)	$d_{\pi-\pi}$ (Å)
K08	21.3	12.5	97	3.3
Ca08	21.8	13.1	103	3.3
Sr08	21.2	12.8	99	3.3
Ba08	21.3	13.0	98	3.3
K16	21.4	13.0	96	3.3
Ca16	22.9	13.6	109	3.2
Sr16	21.9	13.8	97	3.2
Ba16	21.8	14.4	102	3.3

Table S3. Recovery ratio of hydrogels analyzed from continuous strain step experiments (Fig. S9) after 4 cycles. Each measurement was repeated 3 times.

c (M^{n+})	K^+	Ca^{2+}	Sr^{2+}	Ba^{2+}
8 mM	96%	32%	95%	96%
16 mM	91%	20%	60%	57%